

# Optoacoustic signal amplitude and frequency spectrum analysis laser heated bovine liver *ex vivo*

Michelle P. Patterson<sup>1,2</sup>, Christopher B. Riley<sup>3</sup>, Michael C. Kolios<sup>4</sup> and William M. Whelan<sup>1,2</sup>

<sup>1</sup>*Department of Physics, University of Prince Edward Island, Charlottetown (Canada)*

<sup>2</sup>*Department of Biomedical Sciences, Atlantic Veterinary College, Charlottetown (Canada)*

<sup>3</sup>*Animal and Veterinary Sciences, University of Adelaide, Roseworthy (Australia)*

<sup>4</sup>*Department of Physics, Ryerson University, Toronto (Canada)*

**Abstract - Optoacoustic imaging is being investigated as a potential tool for monitoring the onset and progression of laser thermal therapy. In this study OA images were acquired from *ex vivo* bovine liver using a reverse-mode OA imaging system consisting of a pulsed laser operating at 775 nm, and an 8 element annular array ultrasound transducer. LTT was performed with an 810 nm laser at 4 W for five minutes. OA signals were acquired for two minutes prior to, five minutes during, and seven minutes post treatment at a rate of 2 Hz.**

**Treatment induced effects were identified based on the OA signal amplitude in combination with spectral analysis of the OA radio frequency (RF) data. The OA signal amplitude was compared with the measured tissue temperatures. Spectrum analysis commonly performed on ultrasound backscatter RF data, which calculate the spectral midband fit, slope, and intercept of the data was used to quantify the changes in the photoacoustic RF signal.**

**The spectral midband fit and intercept increased on average 11 dB and 10 dB respectively. The amplitude of the OA signals increased during treatment on average 350%. However, post-treatment, the response varied.**

**The results of this study support our hypothesis that LTT causes detectable changes in the amplitude and frequency components of OA signals. Both of these parameters may provide independent information about tissue state. These results demonstrate the potential of OA detection for monitoring LTT.**

## I. INTRODUCTION

### A. Laser Thermal Therapy

Laser Thermal Therapy (LTT) is a minimally invasive technique of destroying diseased tissue. The feasibility of LTT has been demonstrated in a number of sites including breast [5], brain [6, 7], liver [8, 9] and prostate [10, 11]. Thermal therapy involves heating tissue to between 55 and 90 °C for several minutes resulting in cell death. Cell death occurs when thermal damage results in irreversible denaturation of proteins (i.e. coagulation), typically at temperatures above 55°C. Unlike hyperthermia (heating tissue to between 41-45 °C), thermal therapy acts as a stand-alone therapy and does not require further treatment from any additional techniques.

Heating tissues result in highly variable outcomes which can result in insufficient treatment (leading to recurrence) or overly aggressive treatment [12]. This necessitates precise and continuous monitoring during treatment. Real-time monitoring would ensure that the entire tumour has been destroyed while periprostatic critical structures are spared. The efficacy of LTT could be improved if treatment response during treatment could be measured.

Currently, tissue temperatures are commonly being measured during LTT using point sensors (e.g. thermocouples, fluoroptic probes) which provide temperature information at specific locations. Monitoring using point sensors has proven to be inadequate due to the time delay in the conduction of thermal energy from the heating source to the temperature probe. This can result in temperatures exceeding safe limits close to the heating source before they are detected by the temperature probes resulting in undesirable tissue charring.

Tissue temperature can also be monitored using MRI thermometry which provides three-dimensional maps of tissue temperature in real-time. However, this type of monitoring is commonly cost-prohibitive for most treatment centers [3].

### B. Optoacoustic Monitoring of LTT

Optoacoustic (OA) imaging has the potential to provide three-dimensional information in real-time that may offer a means of monitoring the degree of thermal damage to the tissue during LTT. OA imaging takes advantage of the significant changes in tissue optical properties due to thermal coagulation [13]. OA signals are strongly affected by the optical absorption and scattering coefficients, and mechanical properties of the target making coagulation an ideal target for OA imaging. In this study, bovine liver was chosen as an *ex vivo* tissue model because the optical properties of bovine liver are similar to those of a highly vascularized tumour [14]. The optical absorption and reduced scattering coefficients (at 1064 nm) of bovine liver have been shown to increase by upto two- and four-fold, respectively when coagulated [15].

## II. MATERIALS AND METHODS

### A. Imaging protocol

Twenty liver samples obtained from 10 different bovine livers were cut to approximately 2 by 2 cm with 1 cm thickness and sealed inside clear plastic. A sample was placed in the waterbath (maintained at 38°C) of a reverse-mode optoacoustic imaging system (Seno Medical Instruments TX) consisting of an Nd:YAG pumped Ti:Sapphire laser operating at 1064 nm and an 8 element annular array transducer with a central frequency of 4 MHz (Fig. 1). The imaging laser energy was set to 12 mJ during all experiments. The bifurcated fiber bundle and transducer array were positioned 2 cm from the front surface of the liver sample

An 810 nm laser with a maximum power output of 15 W was positioned in the waterbath approximately 2 cm from the back surface of the liver sample, along the same axis as the OA transducer array. This resulted in an illuminated area approximately 1 cm in diameter. The liver irradiation was performed at 4 W for 5 minutes. A fluoroptic temperature probe (Lumasense Technologies, CA) was calibrated using an ice bath following the calibration procedures outlined in the fluoroptic user manual. The probe was placed approximately along the same axis as the center of the 810 nm laser beam and OA transducer on the side of the sample facing the 810 nm laser. Prior to OA imaging the fluoroptic probe was used to ensure that the liver sample had equilibrated to 38°C. During laser heating, the temperature was measured every 1 second. Temperature readings provide a secondary measure of the tissue state during the heating protocol.

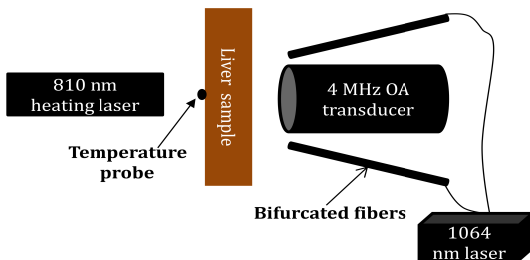


Figure 1: Schematic of the experimental setup.

A-lines (2 signals/second) were acquired along the axis of the 810 nm laser with no temporal averaging. OA signals were acquired prior to, during and post treatment of LTT on *ex vivo* bovine liver.

OA signals were acquired for 2 minutes prior to thermal heating to obtain control/baseline data of the liver sample. The 810 nm laser was then turned on for 5 minutes to create thermal damage in the liver sample during which the OA system continued to acquire A-lines at the same location. The 810 nm laser was then turned off and OA signals continue to be acquired for 7 minutes during which time the temperature of the liver sample decrease to 43°C. (the cutoff temperature for any further thermal damage. A total of 20 liver samples were evaluated.

### B. Data Analysis

For analysis of the OA amplitude the Hilbert transform was applied to all OA signals. The average OA signal obtained prior to thermal heating was divided from all OA signals to remove the baseline signal originating from the untreated tissue. OA signals between 22 mm and 32 mm from the transducer were used. This window excludes the typically strong OA signals obtained from tissue surfaces and includes all signals within the 1 cm tissue sample. An integration of each OA signal between the front and back surface (22 mm and 32 mm) was performed to demonstrate the relative OA signal over the 14 minute acquisition.

The frequency component analysis of the OA data was performed in a similar manner to that of ultrasound tissue characterization using power spectrum analysis [17]. An ROI was chosen so that boundaries of the ROI are all within the investigated tissue (i.e. between 22 mm and 32 mm from the transducer). An ROI representing a 5 mm depth into the treated side of the sample (the approximate depth in which all the samples were damaged) was chosen for analysis. The FFT was applied to the raw RF data and the mean of the squared spectral magnitudes was averaged to obtain a power spectrum. This spectrum was converted to the dB scale.

A negative 160 volt, 6 nsec pulse (UTA-3 Transducer Analyzer, Aerotech, Pittsburgh, USA) was applied to the 4 MHz (central frequency) OA transducer array and the RF signal was received by a 0.2 mm diameter calibrated hydrophone c/w preamp and DC coupler (Precision Acoustics, Dorchester, UK). The hydrophone was mounted on a 3D stepper motor controlled scanning system so that the position of the maximum signal could be found. The FFT of the RF was normalized by the spectral calibration provided by Precision Acoustics and presented as an intensity spectrum. This file was squared to give the power spectrum.

The calibrated power spectrum was subtracted from the power spectrum to remove the effects of the sensitivity of the transducer. A linear fit was applied to the resultant power spectrum between 0.5 and 4.5 MHz (which corresponds to the -6 dB bandwidth of the transducer). The midband fit, intercept and the slope of the linear fit were used for comparison.

## III. RESULTS

Detectable changes were seen in the midband fit and intercept (Fig. 2) as well as in the amplitude of the OA signals (Fig. 3). The uncertainty in the spectral parameters in Fig. 2 are due to the variations between the 20 liver samples obtained from the 10 livers. The midband fit and intercept increased by 11 dB and 10 dB respectively. During post-treatment, as the tissue returned to its initial temperature the midband fit and intercept did not show significant changes. The slope showed little variation, with no obvious trends observed before, during or after heating. The amplitude of the OA signals increased during treatment by 350%. The maximum OA signals for each plot in Fig 3 are shown.

## DISCUSSION AND CONCLUSIONS

Both amplitude and frequency spectrum analysis of OA data may provide independent information about tissue state. The amplitude of the OA signal is largely affected by the optical absorption of the target while the frequency components of the signals may be dependent on physiological properties (e.g. size, spatial distribution and number density) of the absorbing structures in a manner somewhat similar to conventional ultrasound imaging [17, 18]. In this case, we hypothesize that the geometrical arrangement of the vascular tree is linked to this [20]. The red blood cells in the blood vessels are thought to be the main absorbing entities responsible for signals detected photoacoustically at these wavelengths [21].

The OA signals obtained prior to and during heating (Fig 3) demonstrate the potential of OA imaging to monitor LTT in real-time.

The amplitude of the OA signals during heating show a consistent increase when compared to pre-heating signals. However, during the post-heating period, the measured OA signal amplitude does not exhibit a consistent trend. This is likely due to the inconsistent alignment of the OA transducer which was ideally to be directly opposite the center of the 810 nm laser beam. The maximum temperature and damage reached during the course of the experiment would be greatest at the center of the lesion. Therefore, we would expect the OA signal change would be greatest at this location as well. The OA signals may have been acquired closer to the center of the

lesion in the plot on the left (which reached a maximum OA signal of 0.67 a.u.) compared to the plot in the middle (maximum OA signal of 0.48 a.u.) and the plot on the right (maximum OA signal of 0.39 a.u.), which may have been acquired the furthest from the center. The variation in the results post-treatment may be explained by the heat transport within the tissue. When the heating laser is turned off the temperature at the center of the lesion would immediately decrease. However, heat would continue to dissipate outward from the center causing the temperature at the boundaries to decrease less quickly or even possibly increase. These results also give us reason to believe that the amplitude change is not solely dependent on temperature (which causes an increase in the OA signal [19]), as every sample returned to its pre-treatment temperature yet the OA signals did not return to their baseline value. This indicates an irreversible change to the tissue that the OA signal is sensitive to (i.e. coagulation).

The temperature is presented as normalized values as the maximum temperature reached has significant uncertainty due to the placement of the temperature probe (10 C/mm).

Overall the results of this study demonstrate that optoacoustics is sensitive to LTT processes and that heat-induced changes in the amplitude and frequency components (midband fit and intercept) of the OA signals are observable in bovine liver *ex vivo*. These results demonstrate the potential of optoacoustics for monitoring laser thermal therapy.

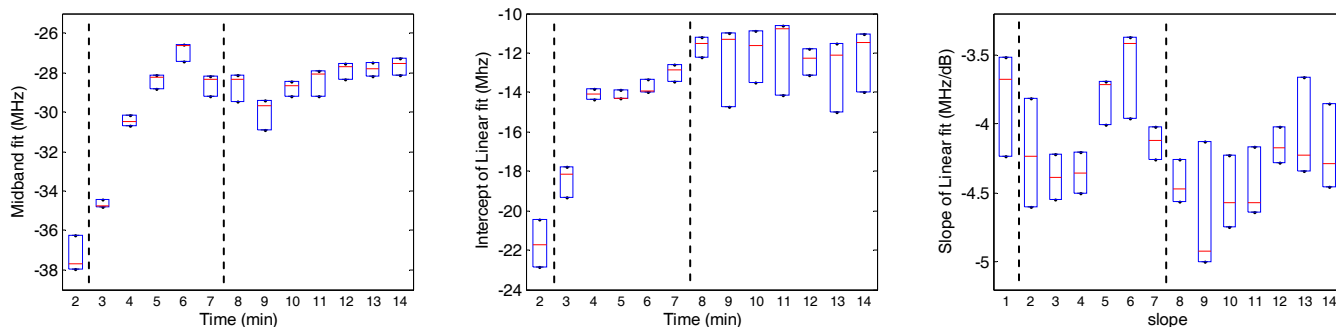


Figure 2: Spectrum analysis parameters (midband fit, intercept and slope) prior to, during and post Laser Thermal Therapy performed on *ex vivo* bovine tissue. Dashed lines represent begin and end of laser heating.

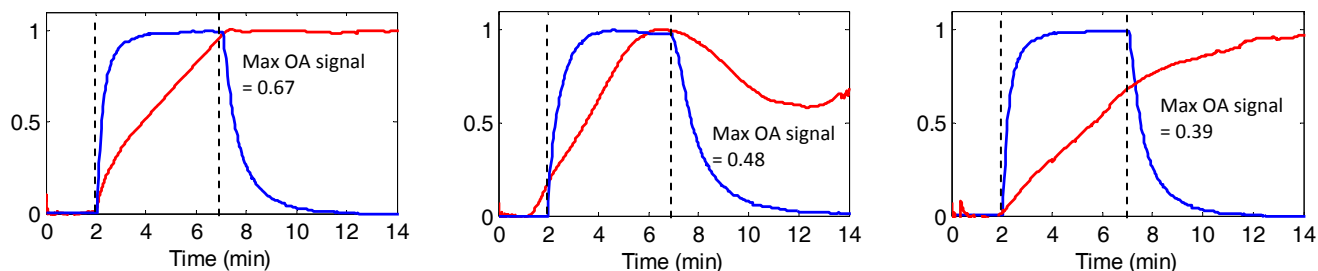


Figure 3: Normalized integrated OA signal (red) and normalized temperature measurements (blue) acquired 2 minutes prior to laser thermal therapy (LTT), 5 minutes during LTT and 7 minutes post LTT. Dashed lines represent begin and end of laser heating.

## REFERENCES

- [1] S. Eggener, P. Scardino, P. Carroll, et al. "Focal therapy for localized prostate cancer: a critical appraisal of rationale and modalities" *Journal of Urology*, **180(2)**, 780-781 (2007).
- [2] D. Bostwick, G. Onik "Inauguration of the prostate cancer focal therapy debate" *Urology*, **70(6)**, S1-S1 (2007).
- [3] Mostafa Atri, Mark Gertner, Masoom Haider, Robert Weersink, John Trachtenberg, "Contrast-enhanced ultrasonography for real-time monitoring of interstitial laser thermal therapy in the focal treatment of prostate cancer" *Canadian Urological Association*, **3(2)**, 125-130 (2009).
- [4] M. Otori, J. Eastham, H. Koh, et al. "Is focal therapy reasonable in patients with early stage prostate cancer (CAP) – an analysis of radical prostatectomy (RP) specimens" *Journal of Urology*, **175:507**, (2006).
- [5] S. Harries, A. Amin, M. Smith, W. Lees, J. Cooke, M. Cook, J. Scurr, M. Kissing, S. Brown "Interstitial laser photocoagulation as a treatment for breast cancer" *British Journal of Surgery*, **81**, 1617-1619 (1994).
- [6] O. Schrottner, P. Ascher, F. Ebner, "Interstitial laser thermotherapy of brain tumour under MRI control" *Proc. Fifth International Congress of the European Laser Association*, 66 (1990).
- [7] F. Roux, L. Merinne, B. Leriche, "Laser interstitial thermotherapy in stereotactical neurosurgery" *Lasers in Medical Science*, **7**, 121-126 (1992).
- [8] J. Hahl, R. Haapiainen, J. Ovaska, P. Puolakkainen, T. Schroder, "Laser-induced hyperthermia in the treatment of liver tumours" *Lasers in Surgery and Medicine*, **10(4)**, 319-321 (1990).
- [9] K. Dowlatshahi, A. Bhattacharya, B. Silver, T. Matalon, J. Williams, "Percutaneous interstitial laser therapy of a patient with recurrent hepatoma in a transplanted liver" *Surgery*, **12(3)**, 603-606 (1992)
- [10] Jason Stafford, Anil Shetty, Andrew Elliot, Sherry Klumpp, Roger McNichols, Ashok Gowda, John Hazle, John Ward, "Magnetic Resonance guided, focal laser induced interstitial thermal therapy in canine prostate model" *The Journal of Urology*, **184 (4)**, 1514-1520 (2010).
- [11] Joshua Stern, Jennifer Stanfield, Wareef Kabbani, Jer-Tsong Hsieh, Jeffrey Cadeddu, "Selective prostate cancer thermal ablation with laser activated gold nanoshells" *The Journal of Urology*, **179 (2)**, 748-753 (2008).
- [12] Benjamin Vakoc, Guillermo Tearney, Brett Bouma, "Real-time microscopic visualization of tissue response to laser thermal therapy" *Journal of Biomedical Optics Letters*, **12(2)**, 020501 (2007).
- [13] W. Whelan, S. Davidson, L. Chin, I. Vitkin, "A novel strategy for monitoring laser thermal therapy based on changes in optothermal properties of heated tissues" *International Journal of Thermophysics*, **26(1)**, 233-241 (2005).
- [14] Wai-Fung Cheong, Scott Prael, Ashley Welch, "A review of optical properties of biological tissues" *IEEE Journal of Quantum Electronics*, **26(12)**, 2166-2185 (1990).
- [15] Annika Nilsson, Christian Stureson, David Liu, Stefan Andersson-Engels, "Changes in spectral shape of tissue optical properties in conjunction with laser-induced thermotherapy" *Applied Optics*, **37(7)**, 1256-1267 (1998).
- [16] J. Eichler, J. Knof, H. Lenz, J. Salk, G. Schafer, "Temperature distribution in tissue during laser irradiation" *Radiation and Environmental Biophysics*, **15**, 277-287 (1978).
- [17] F.L. Lizzi et al. "Theoretical framework for spectrum analysis in ultrasonic tissue characterization" *Journal of Acoustic Society of America* **73(4)**, 1366-1373 (1983).
- [18] F. Lizzi, E. Feleppa, S. K. Alam, and C. X. Deng, "Ultrasonic spectrum analysis for tissue evaluation," *Pattern Recognition Letters* **24**, 637-658 (2003).
- [19] Kirill V. Larin, Irina V. Larina and Rinat O. Esenaliev, "Monitoring of tissue coagulation during thermotherapy using optoacoustic technique" *Journal of Physics D: Applied Physics* **38**, 2645-2643 (2005).
- [20] Jason Zalev, and Michael C. Kolios, "Detecting abnormal vasculature from photoacoustic signals using wavelet-packet features" *Proc. of SPIE*, **7899**, 78992M-1:15 (2011).
- [21] Ratan K. Saha and Michael C. Kolios, "A simulation study photoacoustic signals from red blood cells" *The Journal of the Acoustical Society of America*, **129 (5)**, 2935-2943 (2011).